Author/s:
Di Natale, MR;Patten, L;Molero, JC;Stebbing, MJ;Hunne, B;Wang, X;Liu, Z;Furness, JB

Title:
Organisation of the musculature of the rat stomach

Date:
2022-04-01

Citation:
Di Natale, M. R., Patten, L., Molero, J. C., Stebbing, M. J., Hunne, B., Wang, X., Liu, Z. & Furness, J. B. (2022). Organisation of the musculature of the rat stomach. Journal of Anatomy, 240 (4), pp.711-723. https://doi.org/10.1111/joa.13587.

PROFESSOR JOHN B FURNESS (Orcid ID : 0000-0002-0219-3438)

Article type : Original Paper

# Organisation of the musculature of the rat stomach

Madeleine R Di Natale[1,2], Lauren Patten[2], Juan C Molero[1,2], Martin J Stebbing[1,2], Billie Hunne[1], Xiaokai Wang[3], Zhongming Liu[3], John B Furness[1,2]

[1]Department of Anatomy & Physiology, University of Melbourne, Parkville, VIC 3010, Australia

[2]Florey Institute of Neuroscience and Mental Health, Parkville, VIC 3010, Australia

[3]Department of Biomedical Engineering, University of Michigan, Ann Arbor, MI 48109, USA

*Proofs and Correspondence to:

Dr John B Furness

University of Melbourne

Parkville, VIC 3010

Australia

Email: j.furness@unimelb.edu.au

**Abstract**

The strengths, directions and coupling of the movements of the stomach depend on the organisation of its musculature. Although the rat has been used as a model species to study gastric function, there is no detailed, quantitative study of the arrangement of the gastric muscles in rat. Here we provide a descriptive and quantitative account, and compare it with human gastric anatomy. The rat stomach has three components of the muscularis externa, a longitudinal coat, a circular coat and an internal oblique (sling) muscle in the region of the gastro-esophageal junction. These layers are similar to human. Unlike human, the rat stomach is also equipped with paired muscular esophago-pyloric ligaments that lie external to the longitudinal muscle. There is a prominent muscularis mucosae throughout the stomach and strands of smooth muscle occur in the mucosa, between the glands of the corpus and antrum. The striated muscle of the esophageal wall reaches to the stomach, unlike the human, in which the wall of the distal esophagus is smooth muscle. Thus, the continuity of gastric and esophageal smooth muscle bundles, that occurs in human, does not occur in rat. Circular muscle bundles extend around the circumference of the stomach, in the fundus forming a cap of parallel muscle bundles. This arrangement favours co-ordinated circumferential contractions. Small bands of muscle make connections between the circular muscle bundles. This is consistent with a slower conduction of excitation orthogonal to the circular muscle bundles, across the corpus towards the distal antrum. The oblique muscle merged and became continuous with the circular muscle close to the gastro-esophageal junction at the base of the fundus, and in the corpus, lateral to the lesser curvature. Quantitation of muscle thickness revealed gradients of thickness of both the longitudinal and circular muscle. This anatomical study provides essential data for interpreting gastric movements

**KEYWORDS**

Smooth muscle, gastric motility, corpus, antrum, fundus, gastric ligaments

## 1. INTRODUCTION

A range of disorders of stomach movements affects patients, including gastroparesis, functional dyspepsia, reflux, pyloric stenosis and rapid gastric emptying (Keller et al., 2018, Tack and Pandolfino, 2018, Cheng et al., 2021). These disorders commonly have downstream or associated symptoms, including early post-prandial fullness and satiety, nausea, vomiting, regurgitation, bloating, upper abdominal distension, abdominal pain and weight loss. Because these conditions are common and poorly treated and because co-ordination of gastric movement depends on generation of electrical rhythmicity and electrical conduction, there has been considerable effort made to analyze and model the electrical events on which the movements of the stomach depend (Sanders and Publicover, 1989, Du et al., 2013, Cheng et al., 2021). The conduction of electrical events in the stomach muscle, and the directions and strengths of forces generated when the muscle is excited, depend on the organization of the musculature. However, there is no detailed quantitative data available concerning the organisation of the musculature of the rat stomach, even though this species has been used extensively for physiological studies and investigations of innervation and brain-gut connections (Lentle et al., 2010, Lentle et al., 2016, Lu et al., 2017, Powley et al., 2019, Furness et al., 2020).

In humans and rodents the stomach is made up of three main regions, the fundus (proximal stomach), corpus (the body of the stomach), and antrum (distal stomach tapering towards the duodenum). The proximal stomach acts as a gastric reservoir, while the corpus and antrum are associated with mixing and propulsion of the gastric content. The musculature of the human stomach, a single compartment stomach like rat, has three layers, an external or longitudinal layer beneath which is a circular muscle layer, and an oblique muscle layer that is internal to the circular muscle in the region of the gastro-esophageal junction (Hur, 2020). The oblique muscle curves laterally into the corpus, where it fuses with and becomes continuous with the circular muscle in human. The gastro-esophageal junction differs between species, in particular in relation to whether there is esophageal striated muscle extending to the junction, and whether there is a long intra-abdominal segment of esophagus (McSwiney, 1929). In human, the distal third of the esophagus is smooth muscle; muscle bundles of the wall of the esophagus are continuous with the longitudinal muscle of the gastric wall towards the fundus, and with the circular muscle of the stomach towards the corpus (Hur, 2020). In rat, the distal esophagus is striated muscle and such continuity with gastric muscle, if it occurs, is not obvious (Montedonico et al., 1999). Moreover, the esophageal muscle layers are not longitudinal and circular in the rat, but are arranged as spirals at approximately 90 degrees to each other (Gruber, 1968, Neuhuber et al., 1998).

## 2. MATERIALS AND METHODS

### 2.1 Tissue sources and preparation

All procedures were approved by The Florey Institute of Neuroscience and Mental Heath Animal Ethics Committee. Stomach samples were collected from female and male Sprague Dawley (SD) rats, 6-8 weeks old, 185-206g for females and 220-300g for males. Rats were supplied with food and water ad libitum prior to any experiments. Animals were deeply anesthetised with either an intraperitoneal injection of pentobarbital sodium (100mg/kg) or an intraperitoneal injection of a mixture of ketamine (50 mg/kg) and xylazine (10 mg/kg) prior to being perfused transcardially with phosphate buffered saline (PBS: 0.15 M NaCl, 0.01 M sodium phosphate buffer, pH 7.2) followed by fixative. Varying fixation methods were completed to allow for comparisons, these fixation methods were: 4% paraformaldehyde (Sigma Aldrich, USA), 10% neutral buffered formalin (Trajan, Melbourne, Australia) or Zamboni's fixative (2 % formaldehyde plus 0.2 % picric acid in 0.1 M sodium phosphate buffer, pH 7.0). Some stomach samples were collected from anesthetised rats and placed into PBS containing nicardipine (1 μm) before fixation.

**2.2 Histological staining**

Tissue was placed into histology cassettes and dehydrated through graded ethanol to histolene and embedded in paraffin. Sections (5 μm) were cut and stained with haematoxylin and eosin (H&E) using Leica Autostainer XL and Leica CV5030 coverslipper. Slides were examined and photographed using an Axioplan microscope (Zeiss, Sydney, Australia). Masson's trichrome staining was conducted manually. Sections were then dehydrated, cleared in xylene and coverslipped using permanent mounting media.

**2.3 Histology quantification**

A selection of points, indicated by the pink dots in Figure 6A, were used to measure the thickness of the muscle layers in rat stomach. At each point three measurements of each muscle layer ( longitudinal, circular, oblique (where applicable) and the muscularis mucosa) were taken and averaged. The average was taken for all equivalent fiducial points. Measurements (μm) were completed using Zeiss ZEN software.

**2.3 Immunohistochemistry**

Wholemount preparations were placed in cold fixative (2 % formaldehyde plus 0.2 % picric acid in 0.1 M sodium phosphate buffer, pH 7.0) and incubated overnight at 4°C. Tissues were then washed with dimethyl sulfoxide (DMSO) 3 x 10 minutes and with PBS 3 x 10 minutes. The esophago-pyloric ligament staining was completed as follows: samples were then covered with normal horse serum (10% v/v with triton-X in PBS) and incubated at room temperature (RT) for 1 hour, incubated with mixtures of primary antibodies including sheep anti-neuronal nitric oxide synthase (nNOS; 1:1000, V205: RRID, AB_2314960) (Williamson et al., 1996) and rabbit anti-tachykinin (SKSP1, raised against substance P 1-11; 1:800: RRID, AB_2814842)

(Morris et al., 1986) overnight at RT. The preparations were then washed three times with PBS before a 3 hour incubation with mixtures of secondary antibodies at RT.

The muscle bundle staining was completed as follows: dissected samples were covered with normal horse serum (10% v/v with PBS containing 1% triton-X) and incubated at 37°C for 1 hour, followed by incubation with rabbit anti-α-smooth muscle actin (αSMA; 1;200; AB5694, Abcam, Cambridge, UK: RRID, AB_2223021) overnight at 37°C and for 2 days at RT. The preparations were then washed three times with PBS before a 5 hour incubation with secondary antibody at 37°C.

Cryostat sections to determine muscle bundle widths were prepared as follows. Tissue samples were placed into 30% PBS-sucrose-azide overnight at 4°C followed by overnight in a mixture of OCT compound (Tissue Tek, Elkhart, IN, USA) and PBS-sucrose-azide in a 1:1 ratio before being embedded in 100% OCT and snap frozen in isopentane cooled with liquid nitrogen. Sections (12 μm) were cut and mounted onto SuperFrostPlus® microscope slides (Menzel-Glaser; Thermo Fisher, Scoresby, Vic, Australia). They were air dried for 1 hour then covered with normal horse serum (10% v/v with PBS containing 1% triton-X) and incubated at for 30 minutes at RT, followed by incubation with rabbit anti-α SMA (1:200, overnight at 4°C). The sections were then washed three times with PBS before a 1.5 hour incubation with fluorescent labeled secondary antibody at room temperature.

Following secondary antibody incubation all preparations were then washed three times with PBS before being mounted on standard microscope slides and coverslipped with Dako fluorescence mounting medium (Agilent, Tullamarine, Vic, Australia). Slides were examined and imaged using an Axio Imager microscope (Zeiss, Sydney, Australia) or an LSM800 confocal microscope (Zeiss).

### 2.4 Contrast enhancement and imaging

In order to visualise the circular and longitudinal muscle coats in whole stomach preparations, stomachs underwent prolonged fixation in NBF, for 7 or 14 days. The stomach was then placed in 20 or 80% ethanol for up to a week. Ethanol was replaced with distilled water. This procedure enhanced the outlines of the muscle bundles. These were photographed in whole stomach preparations using oblique illumination to enhance contrast.

## 3. RESULTS

### 3.1 Anatomical features

The overall anatomy of the stomach was examined in vivo, in rats that had been allowed free access to food overnight and which were examined under anesthesia in the morning. The abdomen was opened in the midline and the liver was retracted to reveal the stomach (Figure 1A). The stomach was located to the left in the upper abdomen, and the esophago-gastric junction was to the left of the midline. The same positioning was observed for the stomachs of rats that were perfused with fixative through the heart under deep anesthesia, also after free access to food (Figure 1B). Perfusion with fixative euthanises the rat and the internal organs are preserved in their natural positions. To investigate the regional anatomy as defined by mucosal specialisation, the stomach was removed from freshly killed rats and placed in saline containing the muscle relaxant, nicardipine. It was cut open along the greater curvature from the gastro-esophageal junction to the pyloric sphincter and stretched flat (Figure 1C). Making a 3-dimensional surface 2-dimensional in this way distorts the anatomy, but is useful to illustrate the relationships of the gastric regions.

The main regions of the living stomach in the anesthetised rat and of the opened stomach showed obvious colour differences. The limiting ridge clearly divides the stomach into two regions, proximally the fundus and esophaheal groove that are lined by a stratified squamous epithelium, and distally the corpus and antrum (Figure 1C). The boundary between the corpus and antrum is less clearly defined, which is consistent with there being a zone of transition between the oxyntic mucosa of the corpus and the antral mucosa. There were animal to animal differences in the size of the fundus and in the positioning of the limiting ridge, as also seen in other studies of the rat stomach (Jaffey et al., 2021). However, we could detect no differences in anatomy between stomachs of male and female rats in the weight range that we investigated (185 to 300 g). From 8 perfused stomachs (example in Figure 1B), we created a diagrammatic image for the purpose of mapping gastric features (Figure 1D).

### 3.2 Esophago-pyloric ligaments

The rat possesses a pair of muscular ligaments that extend from a site just lateral to the esophago-gastric junction to the pyloric sphincter (Figure 2).

The ligaments extend from an insertion at the pyloric sphincter to an attachment lateral to the base of the esophagus (Figure 2). They lie parallel and lateral to the mid-line junction of the mesentery of the lesser curvature (lesser omentum). The ligaments are against the gastric surface when the gastric muscle is fully relaxed, but when there is a contractile wave in the antrum, a space is seen between the ligaments and the antral surface (Figure 2B). The extents of the ligaments can be readily revealed by passing a sheet of black plastic underneath (Figure 2C). At the esophageal end, the ligament has a triangular expansion. This is the point of extensive branching of main branches of the left gastric artery (l.g. in Figure 2C) on the ventral and dorsal surfaces (Jaffey et al., 2021). A prominent accumulation of fat, which is also a branching point for

major blood vessels to the corpus region, lies between the ligament and the gastric surface at this point. This has been partly removed in Figure 2C. The esophageal attachment is just lateral to the esophageal groove and merges with the serosa close to where the corpus abuts the fundus, as defined by the limiting ridge (Figure 2D). Figure 2E is an oblique section through the ligament and the surface of the stomach within the region of the esophageal attachment. Between the ligament and the external muscle of the stomach is loose connective tissue (Figure 2E). Immunohistochemistry revealed innervation by axons that were immunoreactive for tachykinins (TK) and neuronal nitric oxide synthase (nNOS; Figure 2F). In other gastric regions, TK immunoreactivity marks the axons of excitatory enteric neurons that innervate the muscle, and nNOS marks axons of enteric inhibitory neurons.

In rat, the ligaments have been referred to as sling muscles (Powley et al., 2012), whereas in human the sling muscle is internal to the gastric wall and is equivalent to the oblique muscle (Spalteholz, 1906, Stein et al., 1995, Zifan et al., 2017, Hur, 2020). Powley et al (2012) found that vagal afferent endings innervate the ligament.

### 3.3 The gastro-esophageal junction

When viewed from the inside of the stomach that has been fixed in situ, the orifice of the distal esophagus at gastro-duodenal junction is almost hidden by closely apposed curves of the limiting ridge (Figure 3A). The orifice can be seen better when the tissue lateral to it is retracted (Figure 3B). The orifice was generally closed in the samples that we examined, as is seen in cross sections taken at the level of the orifice (Figures 3C, F).

In fixed tissue, the most distal part of the esophagus has the darker color typical of striated muscle (Figure 3D) and we confirmed by histology that striated muscle extended to the distal end of the esophagus. The longitudinal muscle of the stomach forms prominent bundles in the region of the fundus approaching the esophagus (Fig 3E). Thick bundles of this longitudinal muscle continue lateral to the distal esophagus at the esophago-gastric junction, and can be readily seen in transverse sections of the junction (Figure 3F and H). The longitudinal muscle at the lessser curvature is also thicker than at more lateral sites. The lateral extents of the esophageal groove are partly obscured by a mucosal fold that includes the limiting ridge (Figure 3A, F), as also described previously (Montedonico et al., 1999).

### 3.4 The circular muscle

The circular muscle is arranged in bundles that run approximately circumferential around the corpus and antrum, and around the fundus (Figure 4).

The lesser curvature is shorter than the greater curvature and to accommodate this difference adjacent bundles coming from the greater curvature coalesce as they approach the lesser curvature. For part of the fundus, circular muscle bundles form rings that involve the greater curvature, but not the lesser curvature (Figure 4A). At the extreme of the fundus, where the gastrophrenic ligament joins, these rings have the appearance of a muscular cap. Thus, this part of the fundus has the anatomical characteristics of a gastric diverticulum. The circular muscle does not follow features of the mucosa, such as the limiting ridge or the boundary between corpus and antrum.

In histological cross sections the circular muscle bundles can be seen to be separated by connective tissue (Figure 4E). Occasionally bands of muscle connect the bundles (Figure 4F), as previously described (Di Natale 2021). The bundles had similar average widths in the antrum and corpus when measured in sections taken at right angles to the lengths of the bundles (Figure 5). They were about half the width in the fundus.

### 3.5 The longitudinal muscle

The longitudinal muscle follows the curve of the stomach (Figure 6) and for most of the gastric surface it is very thin, only about 10-20 μm. On the ventral and dorsal surfaces of the fundus, the muscle turns, creating a curve that looks rather like a fingerprint (Figure 6A, E). Along the greater curvature, to the right of the gastrophrenic ligament, the longitudinal muscle forms parallel thick bundles, that are seen in Fig 3E. Thus in sections parallel to the greater curvature through the region of the gastrophrenic ligament the longitudinal muscle is thicker to the right than to the left (Figure 6B). Some of the thick bundles coalesce and run lateral to the esophago-gastric junction (Figure 6C). The longitudinal bundles follow the length of the antrum, running towards the pyloric sphincter, where they end in close relation to the sphincter muscle (Figure 6D). The longitudinal muscle of the ventral and dorsal surfaces are in direct continuity with the longitudinal muscle of the duodenum.

### 3.6 The oblique (sling) muscle

The oblique muscle forms a crescent around and on the fundic aspect of the gastroesophageal junction (Figure 4B). Its medial margin follows the line of the limiting ridge and it curves laterally to run in the same direction as the circular muscle (Figure 4B), with which it eventually coalesces (Figure 6F). Where the oblique muscle curves around the left side of the esophagus, which is the mid-line of the opened stomach (arrow in Figure 4B), it also merges with and becomes indistinguishable from the circular muscle.

Some bundles of oblique muscle run laterally from their course around the gastroesophageal junction to join the circular muscle after a short distance, whereas other bundles run towards the antrum before curving

laterally to merge with the circular muscle 6-8mm from the medial part of the lesser curvature (Figures 4B. 6Fi-iii).

### 3.7 Muscle associated with the mucosa

A muscularis mucosae at the inner part of the mucosa, external to the submucosal layer, was observed throughout the stomach, and at the base of the esophagus (Figures 3H, 4E, 6F, 7). For most of the stomach it was 30-30 μm thick. It was thicker at the base of the esophagus than in the adjacent stomach (Figure 3H) and was thicker in the fundus than in other regions (Figures 4E, 7). Thin muscle bundles occurred in the mucosa between the glands of the antrum and corpus, but muscle bundles were not observed within the lamina propria of the fundus (Figure 7). The strands of muscle that extend between the glands in the stomach may have a mixing role. In elegant experiments, the pressures in the lumens of gastric glands have been measured and found to oscillate with a rhythm of 4-5 oscillations per min (Synnerstad et al., 1998). Addition of VIP reduced the basal pressure and significantly reduced the amplitudes of oscillations, which is consistent with an innervation of the extension of the muscularis mucosae between the glands by VIP-immunoreactive inhibitory motor neurons.

### 3.8 Relative thicknesses of layers in different regions

The thicknesses of muscle layers and the mucosa throughout the stomach were measured in 2 female and 2 male rats (Figure 8). In some cases a greater number of rats was used. Measurements in Figure 8 are from the ventral wall and the greater and lesser curvatures. The dorsal wall was also examined and appeared identical in structure and dimensions to the ventral wall. For each sample, 3 measurements were taken and averaged to provide the sample mean for that site for the individual rat. The circular and longitudinal muscles varied considerably in thickness throughout the stomach. The circular muscle thickness ranged from 40-60 μm in the middle of the ventral or dorsal surface and towards the greater curvature to 150 μm at the lesser curvature and distal antrum. The longitudinal muscle thickness ranged from 10-20 μm in the mid part and greater curvature of the corpus to 50 μm where it passed dorsal or ventral to the esophago-gastric junction (Figure 6C). The oblique muscle was thickest as it passed the esophagus (adjacent to site O of Figure 8A), with an average of 201.9 ± 29.2 μm. From this site, its thickness decreased at a regular rate until it merged with the circular muscle as it passed around the esophagus (arrow in Figure 4B) and in the corpus (Figure 6Fi-iii). The muscularis musosae was prominent throughout the stomach. In the corpus it averaged 17.9 ± 2.9 μm and in the antrum 22.2 ± 3.3 μm. It was thicker in the fundus, 30.5 ± 4.5 μm.

We also measured the thicknesses of other layers. The mucosa of the fundus had similar thickness throughout this region, with an average thickness of 39.5 ± 5.6 μm. The average thickness of the corpus mucosa was 413.1 ± 63.4 μm and the antral mucosa was 312.9 ± 23.2 μm.

## 4 DISCUSSION

### 4.1 Features of the rat stomach

The gastric muscles of the rat and their relationships are depicted in Figure 9. The rat stomach has paired esophago-pyloric, smooth muscle, ligaments. We also found these in the mouse stomach, but were unable to locate them in human. They are not described in authorative textbooks of human anatomy, such as Gray's Anatomy or in detailed studies of human gastric muscle (Standring, 2016, Hur, 2020). The ligaments insert at one end into the pyloric sphincter and at the other end join the stomach close to the esophago-gastric junction (Figure 9). The ligaments lie against the surface when the stomach is relaxed, but were observed away from the surface when there was a circular muscle contraction of the antrum (Figure 2B). This gives the impression that the ligaments may restrict the separation of the esophago-gastric junction and the pylorus. The muscle of the ligaments was innervated by two types of nerve fibers, those immunoractive for nNOS and those immunoreactive for TK. These are established markers of inhibitory and excitatory neurons that supply gastric muscle in the rat and other species (Furness, 2006), which suggests that tension in the esophago-pyloric ligaments is under neural control, that could contribute to regulation of the length of the lesser curvature (see Figure 9). The external muscle consists of three layers, as in human (Standring, 2016, Hur, 2020), an outer longitudinal muscle, a circular muscle deep to the longitudinal, and an inner oblique (sling) muscle that is closely related to the esophago-gastric junction. There is a prominent muscularis mucosae. Analysis of movements of the rat stomach using spatio-temporal maps indicaes that the muscularis mucosae ungergoes rhythmic, myogenic, contractions (Lentle et al., 2016). We found strands of muscle adjacent to the gastric glands, as has also been reported for human stomach (Arai et al., 2004).

The gastro-esophageal junction in rat and human have distinct differences. Unlike in human (Hur 2020), the circular and longitudinal muscle bundles of the rat stomach are not continuous with muscle bundles that form the wall of the esophagus. This is because the external muscle of the distal esophagus of the rat is composed of spirally arranged striated muscle (Gruber, 1968, Neuhuber et al., 1998), in contrast to the longitudinal and circular smooth muscle coats that occur in human. A number of features may contribute to limiting the passage of content across the junction. The narrowest part of the lumen at the junction is flanked by thickened bundles of longitudinal muscle and circular muscle bundles continuous with those of the corpus

(Figure 3C, H). Contractions of these muscles would reduce the diameter of the gastro-esophageal orifice. Viewed from inside the stomach, mucosal folds obscure the gastro-esophageal orifice (Figure 3A,B) (Montedonico et al., 1999). This would be consistent with the mucosal folds contributing, by a valve-like arrangement, to limiting gastric reflux.

### 4.2 Muscle thickness in different gastric states

The thickness of the muscle was measured from stomachs that were fixed at 10-11 am after free access to food during a 6 pm to 6 am dark phase and during the light phase. The stomachs were full, but the fundus was only moderately distended (Figure 1). Under different conditions, the relative thicknesses of the muscle may have been different. For example, had the fundus been more distended it is anticipated that its muscle layers would have been thinner. The fundus varies the most with meal size, its volume varying from about 400 $mm^3$ in the empty stomach, to about 7000 $mm^3$ in the full stomach (Jaffey et al., 2021). In contrast to this almost 20 fold change in fundic volume, there was an approximately 3-fold difference in antum plus corpus volume.

### 4.3 The arrangement of the circular muscle in bundles

The circular muscle coat is formed by bundles of muscle that wrap around the full circumference of the stomach. Electrical conduction along the bundles is to be expected, based on the smooth muscle of the bundles forming an electrical syncitium. In fact, electrical recordings indicate isochronic occurrence of electrical slow waves around the circumference (Lammers et al., 2009). The slow waves initiate well co-ordinated circular muscle contractile waves (gastric peristalsis), that traverse the corpus and antrum, travelling perpendicular to the circular muscle bundles and partly occluding the lumen (Cannon, 1902, Alvarez and Mahoney, 1922, Lu et al., 2017), although it is interesting to note that the proximal corpus contracts on the side towards the greater curvature but not on the side towards the lesser curvature (Lentle et al., 2016). In the small intestine and colon, conduction of peristaltic events depends on the enteric nervous system (Furness, 2006). Unlike the intestine, the conduction of waves of circular muscle contraction in the longitudinal direction is not impeded by cutting through the myenteric plexus (Cannon, 1912), by blocking excitatory transmission with nicotine (Cannon, 1911), or by preventing nerve action potentials with tetrodotoxin (Lentle et al., 2016). Thus conduction and co-ordination orthogonal to the circular muscle bundles is deduced to be electrical, either through the bands of muscle that connect the circularly arranged bundles (Fig 4F) or through the interstitial cells of Cajal, or through both.

### 4.4 Relations between circular and longitudinal muscle

In the corpus and antrum, the circular muscle was 4-6 times the thickness of the longitudinal muscle. In vivo imaging shows that the dominant movement pattern in these regions are deep circular muscle contractions that partly occlude the lumen and move from the proximal part of the corpus to the distal antrum (Cannon, 1898, Lu et al., 2017). The longitudinal muscle may have a role to restrict the circular muscle contractions being translated into elongation of the corpus and antrum. This appears to be its role in the intestine. When the circular muscle contracts and shortens, it thickens. Were that thickening to be predominantly in the longitudinal direction of the distal stomach, the gut would lengthen and the occlusion of the lumen would be reduced. In the intestine, the longitudinal muscle contracts at the same time as the circular, restricting lengthening and accentuating luminal occlusion. The simultaneous contraction of the two muscle layers was reported during propulsive contractions of the canine intestine in vivo (Bayliss and Starling, 1899) and has also been noted in the esophagus (Roman, 1982, Mittal et al., 2005) and in other intestinal regions and species (Smith and Robertson, 1998). Simultaneous electrical records from the two muscle layers also indicate that slow waves occur in synchrony (Suzuki et al., 1986). When a peristaltic reflex is induced by an imposed increase in intraluminal pressure, it is observed that the contraction of the longitudinal muscle begins slightly before that of the circular (Trendelenburg, 1917). This has been called the preparatory contraction of the longitudinal muscle. In response to suggestions that there may be reciprocal movements of the longitudinal and circular layers (that is, the longitudinal muscle relaxes and the intestine lengthens when the circular muscle contracts), the relationship between their contractions has been examined, and the literature reviewed (Smith and Robertson, 1998). These authors confirmed that the two layers contract together during propulsive reflexes of the intestine. Imaging methods to reveal $Ca^{2+}$ transients in the muscle also show that the two layers are excited at the same time when motility reflexes are initiated (Stevens et al., 2000). In the antrum and corpus of the rat stomach, the longitudinal and circular muscles contract and relax at the same time during slow wave activity (Lentle et al., 2016), with the longitudinal contraction starting slightly before the circular, as in the intestine. The gastric fundus relaxes in both the direction of the longitudinal muscle and in the direction of the circular muscle to accommodate greater volumes of food (Jaffey et al., 2021).

There are instances in which recordings from the intestine show that the longitudinal muscle layer elongates at the same time that the circular muscle contracts (Sarna, 1993, Grider, 2003). It is possible that when the contraction of the circular muscle is sufficiently strong it can overcome the longitudinal muscle contraction and force the longitudinal layer to lengthen. Nevertheless, the literature does indicate that force generated by longitudinal muscle restricts elongation when the circular muscle contracts.

**4.5 Conclusions**

The muscularis externa of the rat stomach has many similarities with human, consisting of an external longitudal and internal circular muscle for most of its extent. In the region of the gastro-esophageal junction there is a further layer, internal to the circular muscle, the oblique or sling muscle, similar again to human. Significant differences from human are the presence of the paired esophago-pyloric ligaments in rat but not human, and differences in the structure of the gastro-esophageal junction. The rat and human are also similar in the innevation of the gastric smooth muscle, in both cases being supplied by nitrergic inbitory innervation and excitatory neurons with the primary neurotransmitter being ACh (Furness et al., 2020). Regional differences in muscle thickness suggest that the strengths of contraction differ by region. The circumferential arrangement of the circular muscle bundles, and the small bands of muscle that connect adjacent bundles, are consistent with rapid circumferential conduction of excitation and slower conduction orthoganol to the bundles. The quantitative data that has been obtained in this study is expected to enhance modelling of gastric function (Cheng et al. 2021).

**Acknowledgements**:

We thank Gavan Mitchell of the Imaging Unit, University of Melbourne for assitance with photography. Confocal microscopy was undertaken at the Biological Optical Microscopy Platform, University of Melbourne. This study utilised the Phenomics Australia Histopathology and Slide Scanning Service, University of Melbourne. We thank Tina Cardamone of the Service for her assistance and advice.

**Funding information**

This work was supported by NIH (SPARC) grant, The Virtual Stomach (OT2OD030538), Principal Investigators Leo Cheng (University of Auckland) and ZL (University of Michigan) and NIH (SPARC) grant ID # OT2OD023847 (Principal Investigator Terry Powley, Pudue University).

**Data Availability**.

The data that support the findings of this study are openly available in the NIH SPARC DATCORE: DOI: 10.26275/tlgo-dfke

**Author contributions**

JBF and MRDT conceived and designed the study; MRDT, LP, BH and JBF performed experiments; JBF, XW, ZL and MRDT analyzed data and interpreted results of experiments; JBF and MRDT prepared figures, JCM and MJS provided tissue specimens; JBF wrote the manuscript; JBF and MRDT edited and revised the manuscript; all authors have approved the final version of the manuscript.

## Conflict of Interest

The authors declare no conflict of interest

## References


Alvarez, W. C. & Mahoney, L. J. 1922. Action currents in stomach and intestine. *American Journal of Physiology,* 58**,** 476-493.

Arai, K., Ota, H., Hidaka, E., Hayama, M., Sano, K., Sugiyama, A., Akamatsu, T. & Katsuyama, T. 2004. Histochemical, ultrastructural, and three-dimensional observation of smooth muscle cells in human gastric mucosa. *Histochemistry and Cell Biology,* 121**,** 229-237.

Bayliss, W. M. & Starling, E. H. 1899. The movements and innervation of the small intestine. *Journal of Physiology (London),* 24**,** 99-143.

Cannon, W. B. 1898. The movements of the stomach studied by means of the Roentgen rays. *American Journal of Physiology,* 1**,** 359-382.

Cannon, W. B. 1902. The movements of the intestines studied by means of the Roentgen rays. *American Journal of Physiology,* 6**,** 251-277.

Cannon, W. B. 1911. *The mechanical factors of digestion,* London, Edward Arnold.

Cannon, W. B. 1912. Peristalsis, segmentation and the myenteric reflex. *American Journal of Physiology,* 30**,** 114-128.

Cheng, L. K., Nagahawatte, N. D., Avci, R., Du, P., Liu, Z. & Paskaranandavadivel, N. 2021. Strategies to refine gastric stimulation and pacing protocols: experimental and modeling approaches. *Frontiers in Neuroscience,* 15**,** 645472.

Du, P., O'grady, G., Gao, J., Sathar, S. & Cheng, L. K. 2013. Toward the virtual stomach: progress in multiscale modeling of gastric electrophysiology and motility. *Wiley Interdisciplinary Reviews: Systems Biology and Medicine,* 5**,** 481-493.

Furness, J. B. 2006. *The Enteric Nervous System,* Oxford, Blackwell.

Furness, J. B., Di Natale, M., Hunne, B., Oparija-Rogenmozere, L., Ward, S. M., Sasse, K. C., Powley, T. L., Stebbing, M. J., Jaffey, D. & Fothergill, L. J. 2020. The identification of neuronal control pathways supplying effector tissues in the stomach. *Cell and Tissue Research,* 382**,** 433-445.

Grider, J. R. 2003. Reciprocal activity of longitudinal and circular muscle during intestinal peristaltic reflex. *American Journal of Physiology,* 284**,** G768-G775.

Gruber, H. 1968. Structure and innervation of the striated muscle fibres of the esophagus of the rat. *Zeitschrift für Zellforschung,* 91**,** 236-247.

Hur, M.-S. 2020. Muscular architecture of the abdominal part of the esophagus and the stomach. *Clinical Anatomy,* 33**,** 530-537.

Jaffey, D. M., Chesney, L. & Powley, T. L. 2021. Stomach serosal arteries distinguish gastric regions of the rat. *Journal of Anatomy,* 00**,** 1-10.

Keller, J., Bassotti, G., Clarke, J., Dinning, P., Fox, M., Grover, M., Hellström, P. M., Ke, M., Layer, P., Malagelada, C., Parkman, H. P., Scott, S. M., Tack, J., Simren, M., Törnblom, H. & Camilleri, M. 2018. Advances in the diagnosis and classification of gastric and intestinal motility disorders. *Nature Reviews Gastroenterology & Hepatology,* 15**,** 291-308.

Lammers, W. J. E. P., Ver Donck, L., Stephen, B., Smets, D. & Schuurkes, J. a. J. 2009. Origin and propagation of the slow wave in the canine stomach: the outlines of a gastric conduction system. *American Journal of Physiology-Gastrointestinal and Liver Physiology,* 296**,** G1200-G1210.

Lentle, R. G., Janssen, P. W. M., Goh, K., Chambers, P. & Hulls, C. 2010. Quantification of the effects of the volume and viscosity of gastric contents on antral and fundic activity in the rat stomach maintained ex vivo. *Digestive Diseases and Sciences,* 55**,** 3349-3360.

Lentle, R. G., Reynolds, G. W., Hulls, C. M. & Chambers, J. P. 2016. Advanced spatiotemporal mapping methods give new insights into the coordination of contractile activity in the stomach of the rat. *American Journal of Physiology-Gastrointestinal and Liver Physiology,* 311**,** G1064-G1075.

Lu, K.-H., Cao, J., Thomas Oleson, S., Powley, T. L. & Liu, Z. 2017. Contrast-enhanced magnetic resonance imaging of gastric emptying and motility in rats. *IEEE Transactions on Biomedical Engineering,* 64**,** 2546-2554.

Mcswiney, B. A. 1929. The structure and movements of the cardia. *Quarterly Journal of Experimental Physiology* 19**,** 237-241.

Mittal, R. K., Liu, J., Puckett, J. L., Bhalla, V., Bhargava, V., Tipnis, N. & Kassab, G. 2005. Sensory and motor function of the esophagus: Lessons from ultrasound imaging. *Gastroenterology,* 128**,** 487-497.

Montedonico, S., Godoy, J., Mate, A., Possögel, A. K., Diez-Pardo, J. A. & Tovar, J. A. 1999. Muscular architecture and manometric image of gastroesophageal barrier in the rat. *Digestive Diseases and Sciences,* 44**,** 2449-2455.

Morris, J. L., Gibbins, I. L., Campbell, G., Murphy, R., Furness, J. B. & Costa, M. 1986. Innervation of the large arteries and heart of the toad Bufo marinus by adrenergic and peptide-containing neurons. *Cell and Tissue Research,* 243**,** 171-184.

Neuhuber, W. L., Kressel, M., Stark, A. & Berthoud, H.-R. 1998. Vagal efferent and afferent innervation of the rat esophagus as demonstrated by anterograde DiI and DiA tracing: focus on myenteric ganglia. *J. Auton. Nerv. Syst.,* 70**,** 92-102.

Powley, T. L., Gilbert, J. M., Baronowsky, E. A., Billingsley, C. N., Martin, F. N. & Phillips, R. J. 2012. Vagal sensory innervation of the gastric sling muscle and antral wall: implications for gastro-esophageal reflux disease? *Neurogastroenterology and Motility,* 24**,** e526-e537.

Powley, T. L., Jaffey, D. M., Mcadams, J., Baronowsky, E. A., Black, D., Chesney, L., Evans, C. & Phillips, R. J. 2019. Vagal innervation of the stomach reassessed: brain-gut connectome uses smart terminals. *Annals of the New York Academy of Sciences,* 1454**,** 14-30.

Roman, C. 1982. Nervous control of esophageal and gastric motility. *In:* BERTACCINI, G. (ed.) *Handbook of Experimental Pharmacology: Mediators and drugs in gastrointestinal motility.* Berlin: Springer-Verlag.

Sanders, K. M. & Publicover, N. G. 1989. Electrophysiology of the gastric musculature. *In:* WOOD, J. D. (ed.) *Handbook of Physiology: The Gastrointestinal System.* 2 ed. Baltimore, MD: American Physiology Society.

Sarna, S. K. 1993. Gastrointestinal longitudinal muscle contractions. *American Journal of Physiology,* 265**,** G156-G164.

Smith, T. K. & Robertson, W. J. 1998. Synchronous movements of the longitudinal and circular muscle during peristalsis in the isolated guinea-pig distal colon. *Journal of Physiology (London),* 506**,** 563-577.

Spalteholz, W. 1906. *Hand-atlas of human anatomy; edited and translated from the 4th German edition by Lewellys F. Barker,* Philadelphia, Lippincott.

Standring, S. 2016. *Gray's Anatomy: The anatomical basis of clinical practice.,* New York, Elsevier/Churchill Livingstone.

Stein, H. J., Liebermann-Meffert, D., Demeester, T. R. & Siewert, J. R. 1995. Three-dimensional pressure image and muscular structure of the human lower esophageal sphincter. *Surgery,* 117**,** 692-698.

Stevens, R. J., Publicover, N. G. & Smith, T. K. 2000. Propagation and neural regulation of calcium waves in longitudinal and circular muscle layers of guinea pig small intestine. *Gastroenterology,* 118**,** 892-904.

Suzuki, N., Prosser, C. L. & Dahms, V. 1986. Boundary cells between longitudinal and circular layers: essential for electrical slow waves in cat intestine. *American Journal of Physiology,* 250**,** G287-G294.

Synnerstad, I., Ekblad, E., Sundler, F. & Holm, L. 1998. Gastric mucosal smooth muscles may explain oscillations in glandular pressure: role of vasoactive intestinal peptide. *Gastroenterology,* 114**,** 284-294.

Tack, J. & Pandolfino, J. E. 2018. Pathophysiology of gastroesophageal reflux disease. *Gastroenterology,* 154**,** 277-288.

Trendelenburg, P. 1917. Physiologische und pharmakologische Versuche über die Dünndarmperistaltik. *Naunyn Schmiedeberg's Arch. Exp. Path. Pharmak.,* 81**,** 55-129.

Williamson, S., Pompolo, S. & Furness, J. B. 1996. GABA and nitric oxide synthase immunoreactivities are colocalized in a subset of inhibitory motor neurons of the guinea-pig small intestine. *Cell and Tissue Research,* 284**,** 29-37.

Zifan, A., Kumar, D., Cheng, L. K. & Mittal, R. K. 2017. Three-dimensional myoarchitecture of the lower esophageal sphincter and esophageal hiatus using optical sectioning microscopy. *Scientific Reports,* 7**,** 13188.

**Figure Descriptions**

FIGURE 1: Anatomy of the rat stomach. A: The stomach in a living, anesthetised rat. The rat has been opened in the ventral midline and the liver has been retracted into the abdominal cavity. A black plastic membrane was placed under the fundus and corpus for image contrast. B: The stomach that has been removed from a rat that was perfused through the heart. C: Fresh stomach opened along the greater curvature and stretched flat. We have used the terms 'medial' and 'lateral' to refer to positions in the opened stomach. D: This diagrammatic image used for mapping features is based on stomachs from perfused rats (as in B).

FIGURE 2: The esophago-pyloric ligaments. A: Diagram to show the position of the ventral ligament. B: The ligament as it appears when there is a deep peristaltic contraction of the antrum. The ligament lifts away from the gastric surface. C: Both ligaments are in this image of the freshly dissected, unfixed stomach. The dorsal ligament is difficult to see against the gastric surface. The ventral ligament is revealed more clearly when a black plastic membrane is placed beneath it. D: Esophageal attachment of the ventral ligament (fixed flattened stomach). The attachment is onto the gastric surface lateral to the esophageal groove and the esophagus. E: Section through the ligament at its attachment close to the distal esophagus. The ligament is composed of smooth muscle. Its join to the gastric surface is fibro-muscular (H & E staining). F: Nerve fibers immunoreactive for nNOS and tachykinins (TK) innervating the ligament.

FIGURE 3: The gastro-esophageal junction. A: The junction seen from within the stomach in a preparation that was fixed after removal and dissection in saline. The limiting ridge obscures the orifice of the esophagus. The positions of the sections F (F) and G (G) are indicated. This is the most common appearance: the folds of mucosa where the esophagus meets the stomach obscure the opening into the esophagus. B: The same stomach as in A, with the limiting ridges retracted to reveal the esophageal orifice. C: The narrow opening at the most distal end of the esophagus seen in a sagittal section view of the junction. D: The base of the esophagus has the color typical of striated muscle, in comparison to the lighter color of

the gastric wall. E: The bundles of longitudinal muscle of the greater curvature near the esophago-gastric junction. Some bundles pass lateral to the esophagus (asterisks) and can be seen in the section of panel F (enlarged in H). The dotted line marks the midline of the greater curvature of the fundus. F: Cross section through the esophago-gastric junction at the level of the esophageal orifice (position of section shown in panel A). At the junction, the esophageal groove is narrowed, and is bounded laterally by the mucosa of the corpus and the limiting ridge (LR). G: Section adjacent to the esophago-gastric junction, at (G) in panel A. The lips of the groove formed by the limiting ridge are apparent. H: Enlargement of the boxed region of panel F. This shows the thickened longitudinal muscle of the stomach that skirts the esophago-gastric junction. F and H stained with hematoxylin and eosin, G with trichrome.

FIGURE 4. Arrangement of the circular muscle. A: The organisation of circular muscle bundles when visualised in the whole stomach. B: The circular muscle as seen in an opened, flattened stomach, and the relation to the oblique muscle (red). Towards midline, and laterally, the oblique muscle fuses with the circular muscle (red arrows). C, D: Contrast enhanced images of the circular muscle of the corpus (C) and fundus (D) in preparations of whole stomach treated with prolonged fixation and ethanol to reveal the muscle bundles and the connective tissue (lighter color) between bundles. E: Section showing circular muscle bundles in the fundus in transverse section, separated by connective tissue (trichrome stain). F: Image of circular muscle bundles in a wholemount stained with anti-α-smooth muscle actin (α SMA). Muscle bundles were connected by bands of smooth muscle cells.

FIGURE 5. Widths of circular muscle bundles. The bundles were measured from cross sections taken from the ventral stomach which were stained with anti-α-smooth muscle actin (αSMA) immunohistochemistry. An example of the staining is shown in Figure 7.

FIGURE 6: The longitudinal muscle and the merging of the oblique muscle. A: Arrangement of the longitudinal muscle and sites of images. The thicker lines indicate muscle thickening. B: Section running right to left and including the base of the gastro-phrenic ligament. The longitudinal muscle to the right, that runs towards the esophago-gastric junction, is thicker than the longitudinal muscle to the left of the ligament. The thickened muscle bundles to the right are also seen in Fig 3E. C: The thickening of the longitudinal muscle as it passes lateral to the esophago-gastric junction. D: The pyloric sphincter. The section shows the longitudinal muscle of the stomach merging with the sphincter. In the first part of the duodenum large glands of Brunner are prominent in the submucosa. E: Contrast enhanced image of the site where the longitudinal muscle turns back on itself. Image from whole fixed stomach using oblique illumination. F: Sections taken in a line along the line marked by the bar in panel A. Closest to the esophago-gastric junction, (Fi), the circular and oblique layers are distinct, further away, (Fii), they come close together and towards the mid-

point of the stomach the two layers become one (Fiii). B, C, D: hematoxylin and eosin; F: Masson's trichrome; E: unstained.

FIGURE 7. The muscularis mucosae. Stomach preparations from the ventral fundus (A), corpus (B) and antrum (C) were stained with anti- α smooth muscle actin (αSMA). The muscularis mucosae, muscularis externa and smooth muscle compoments of the muscularis mucosae that extend between the mucosal glands are stained.

FIGURE 8. A: Points of measurement of thicknesses of the layers of the rat stomach. B, C: Circular muscle and longitudinal muscle thicknesses at the sites from which measurements were taken. D: Mean values for thicknesses of all layers ± SEM. Measurements are from a minimum of 2 female and 2 male rats.

FIGURE 9. The muscles of the rat stomach, their directions and relationships. The external muscle of the rat stomach has two complete layers, the longitudinal and circular layers and an incomplete layer, the oblique muscle. It also has a muscularis mucosae, not illustrated, that lies adjacent to the lining mucosa throughout the stomach, and paired muscular ligaments, the esophago-pyloric ligaments.

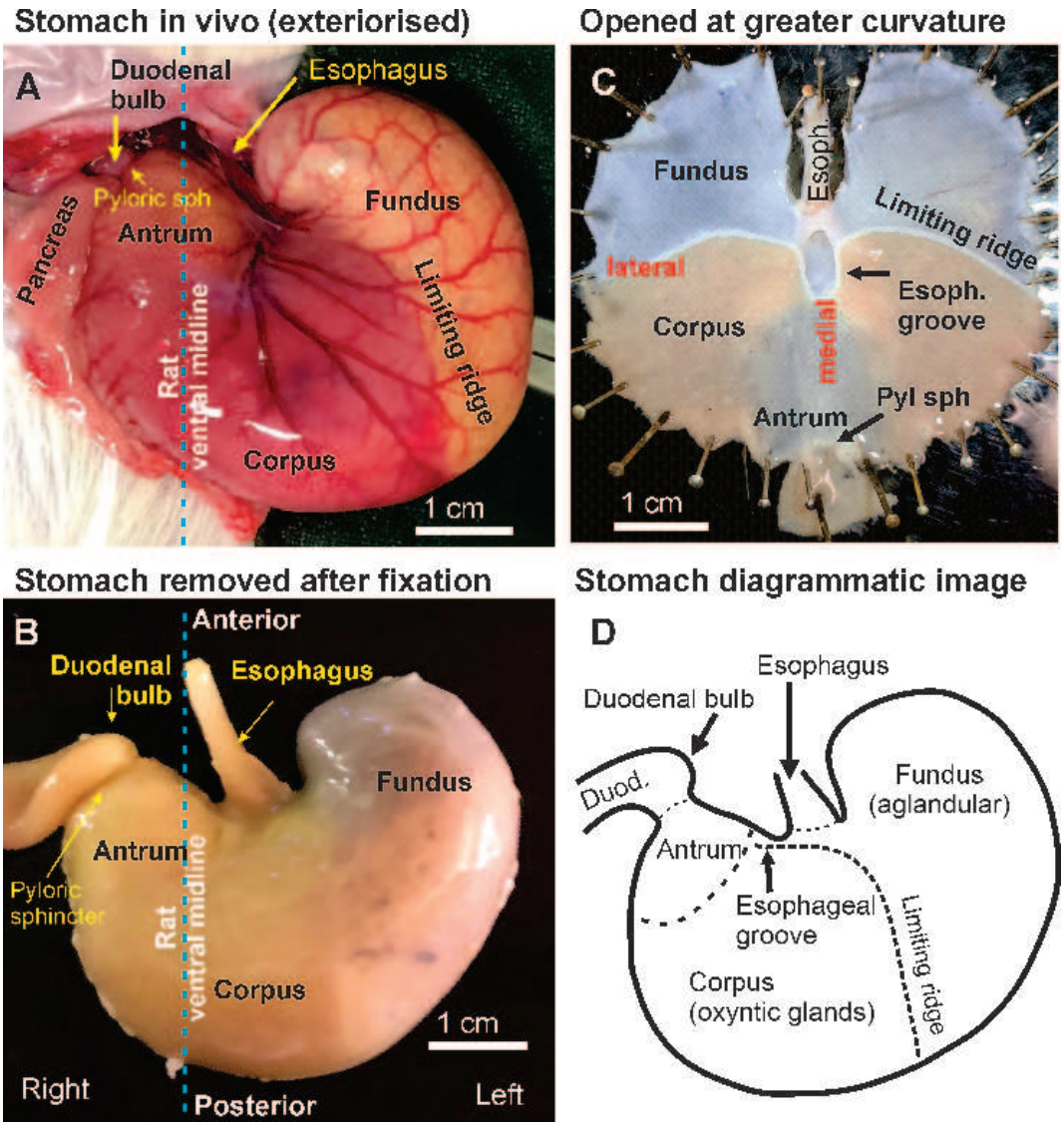


joa_13587_f1.tif

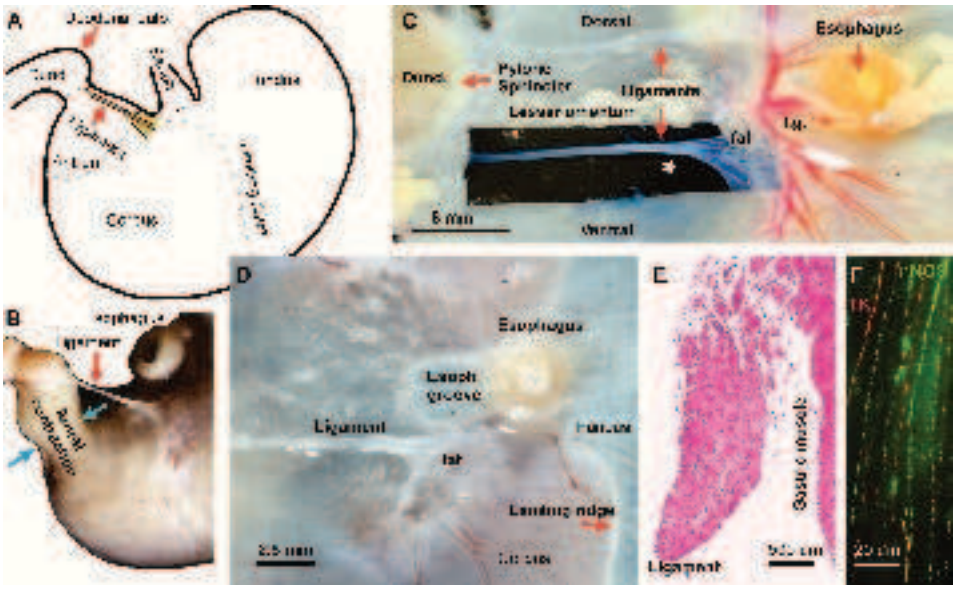


joa_13587_f2.tif

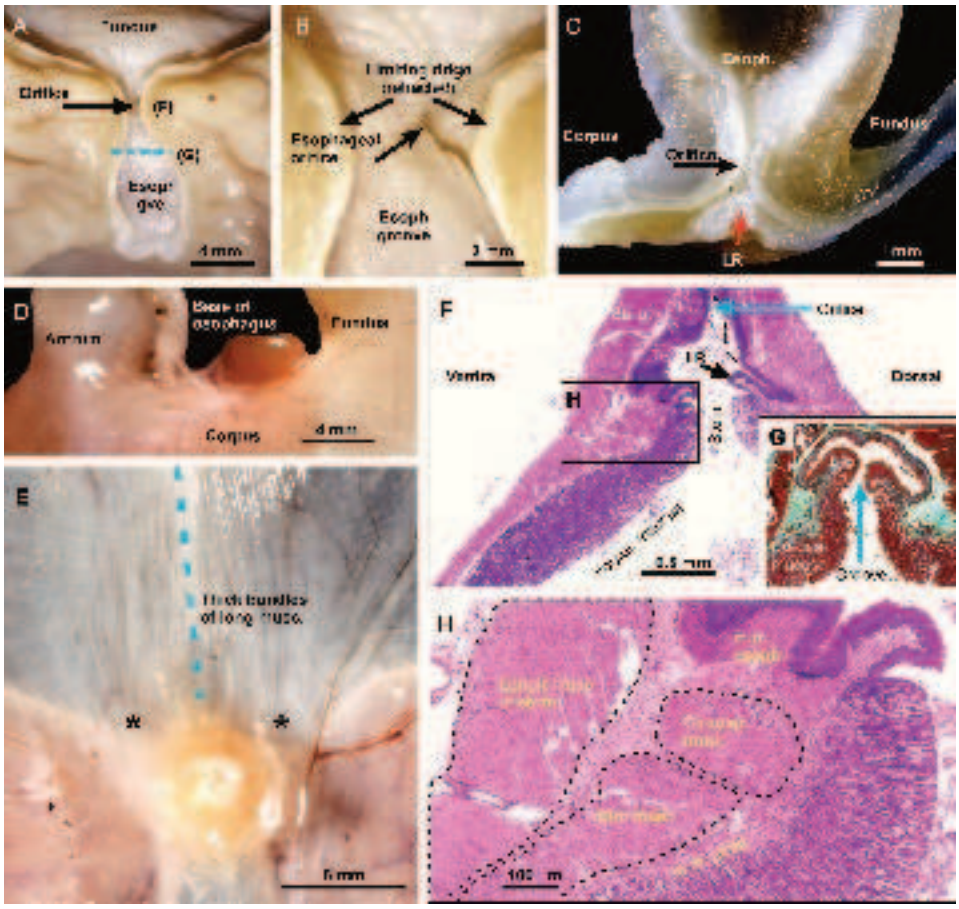


joa_13587_f3.tif

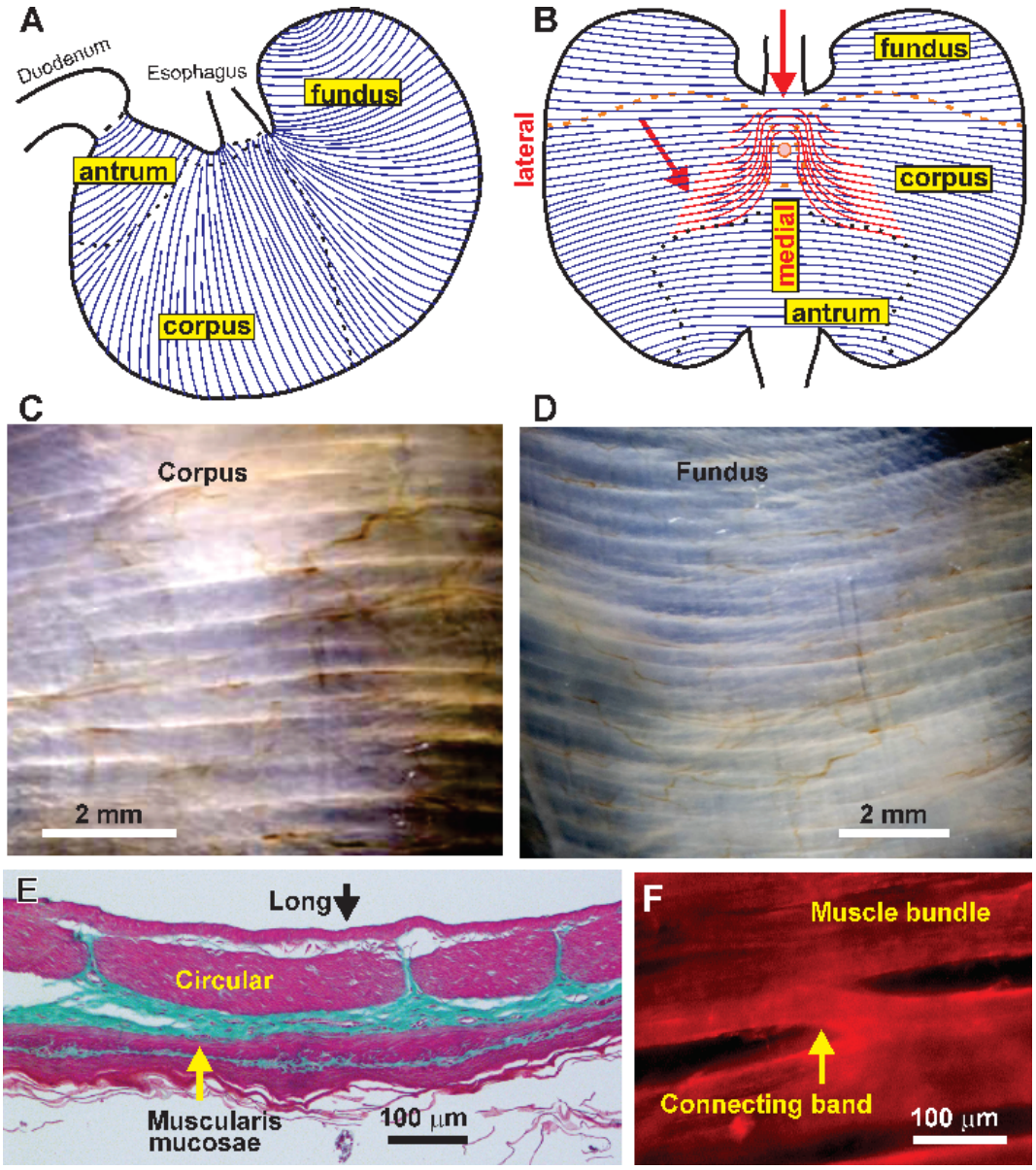


joa_13587_f4.tif

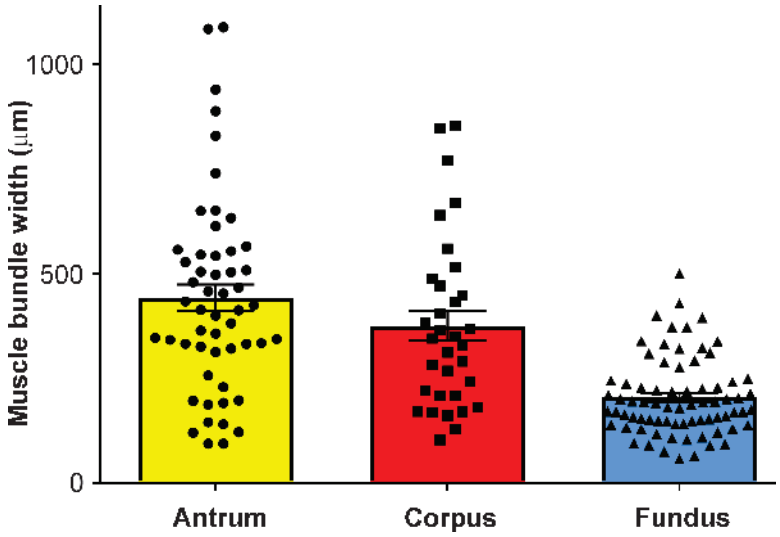


joa_13587_f5.tif

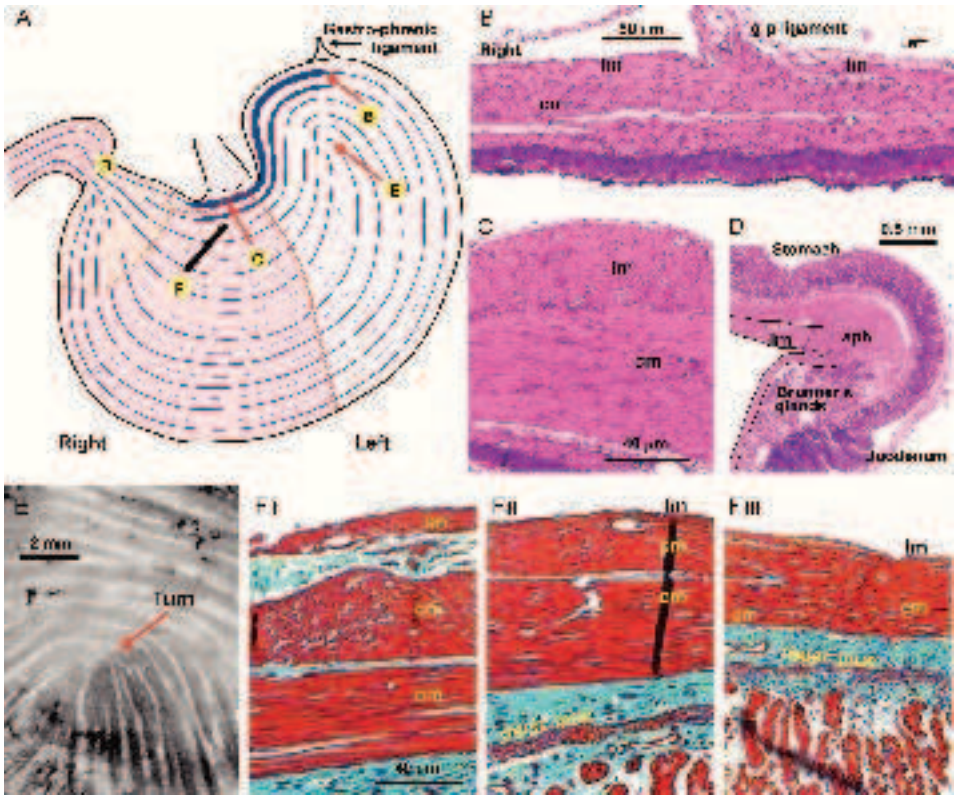


joa_13587_f6.tif

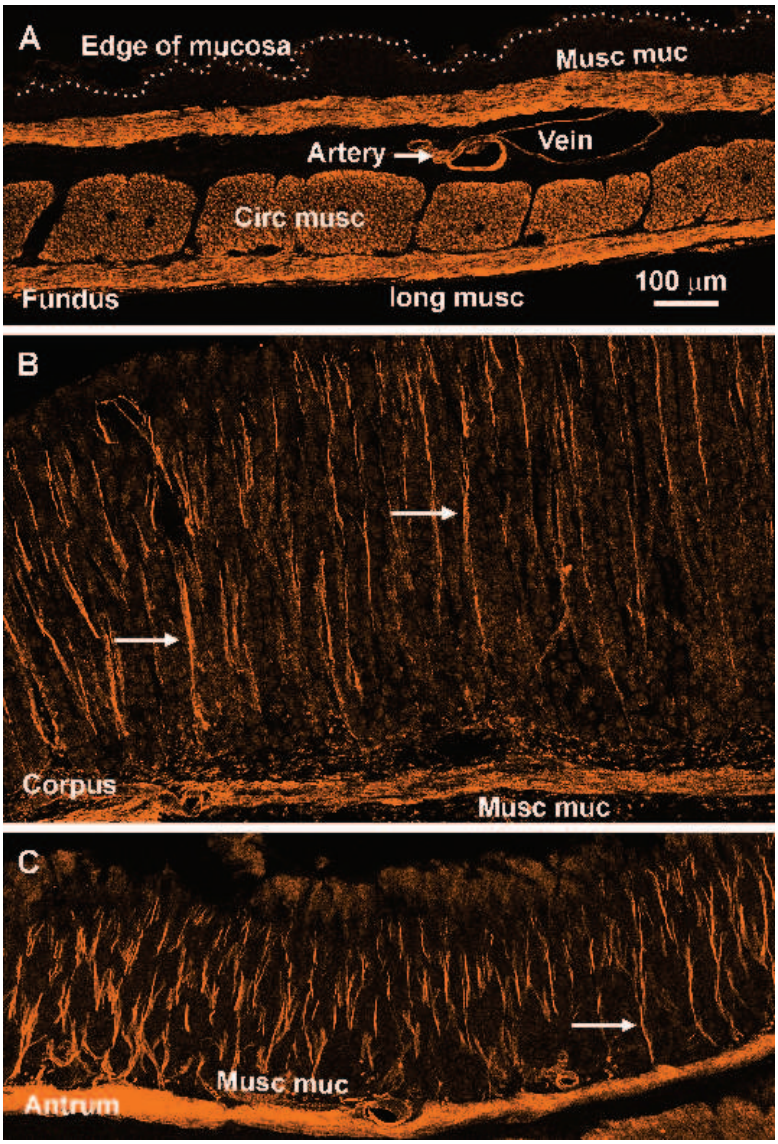


joa_13587_f7.tif

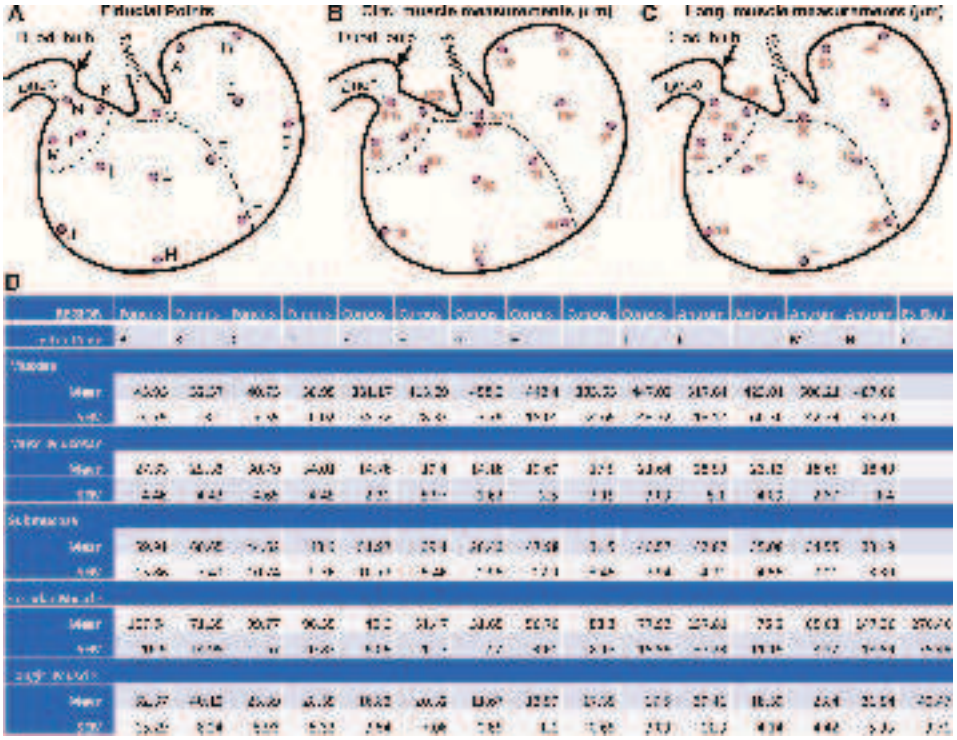

joa_13587_f8.tif

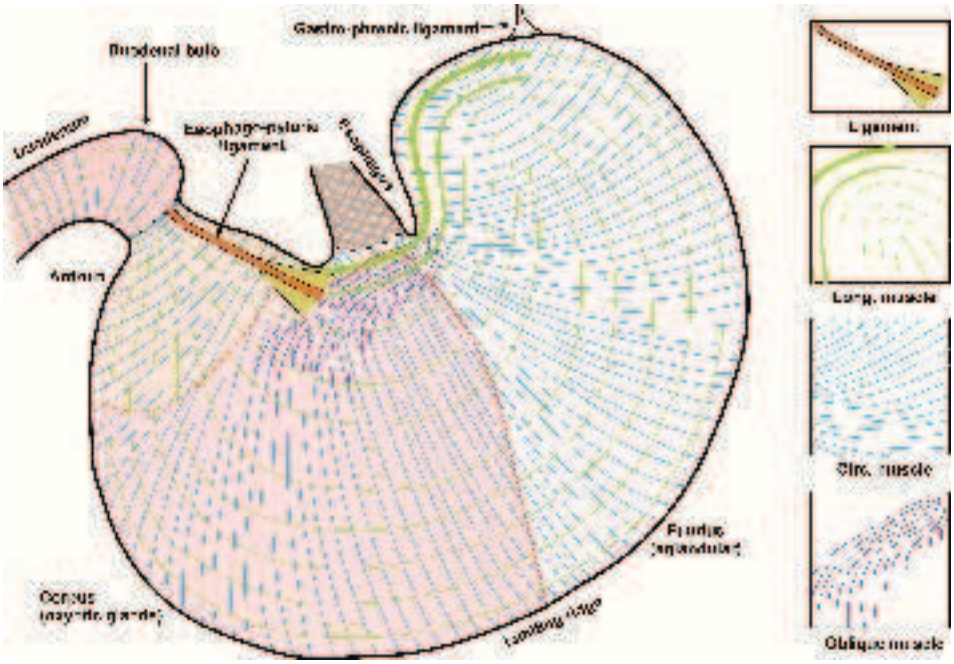


joa_13587_f9.tif